The Journal of Immunology

The Immunosuppressor Mycophenolic Acid Kills Activated Lymphocytes by Inducing a Nonclassical Actin-Dependent Necrotic Signal

Benjamin Chaigne-Delalande, Gwendaline Guidicelli, Lionel Couzi, Pierre Merville, Walid Mahfouf, Stéphane Bouchet, Mathieu Molimard, Benoit Pinson, Jean-François Moreau and Patrick Legembre

J Immunol 2008; 181:7630-7638; ;
doi: 10.4049/jimmunol.181.11.7630
http://www.jimmunol.org/content/181/11/7630

The Journal of Immunology is published twice each month by
The American Association of Immunologists, Inc.,
1451 Rockville Pike, Suite 650, Rockville, MD 20852

Print ISSN: 0022-1767 Online ISSN: 1550-6606.

The Immunosuppressor Mycophenolic Acid Kills Activated Lymphocytes by Inducing a Nonclassical Actin-Dependent Necrotic Signal[1]

Benjamin Chaigne-Delalande,[2]*†‡ Gwendaline Guidicelli,[2]*†‡§ Lionel Couzi,*†‡§ Pierre Merville,*‡§ Walid Mahfouf,*†‡ Stéphane Bouchet,*¶‖ Mathieu Molimard,*¶‖ Benoit Pinson,*# Jean-François Moreau,*†‡§ and Patrick Legembre[3]*†‡

Mycophenolate mofetil (MMF) is an immunosuppressive agent used in transplantation. Over the last decade, MMF has also emerged as an alternative therapeutic regimen for autoimmune diseases, mainly for patients refractory to other therapies. The active compound of MMF, mycophenolic acid (MPA), depletes the intracellular pool of guanosine tri-phosphate through inosine monophosphate dehydrogenase blockade. The molecular mechanism involved in the elimination of T and B lymphocytes upon inhibition of inosine monophosphate dehydrogenase remains elusive. In this study, we showed that in contrast to the immunosuppressors azathioprine, cyclosporin A, and tacrolimus, MPA killed lymphocytes through the activation of a caspase-independent necrotic signal. Furthermore, the MPA-mediated necrotic signal relied on the transmission of a novel intracellular signal involving Rho-GTPase Cdc42 activity and actin polymerization. In addition to its medical interest, this study sheds light on a novel and atypical molecular mechanism leading to necrotic cell death. ***The Journal of Immunology,*** **2008, 181: 7630–7638.**

Inosine 5′-monophosphate dehydrogenase (IMPDH)[4] is the rate-limiting enzyme in the de novo pathway for the synthesis of GTP (see Fig. 1*A*). Mycophenolate mofetil (MMF) is a prodrug that is metabolized into its active moiety termed mycophenolic acid (MPA) and is widely used to prevent rejection of kidney allografts in recipients (1, 2). MPA is a specific and noncompetitive inhibitor of IMPDH. IMPDH inhibition drives a depletion of GTP that alters processes such as DNA replication, transcription, and protein translation and hence leads to a G_1/S cell cycle arrest. In addition, the GTP depletion impairs the transfer of fucose and mannose to glycoproteins and reduces the expression of adhesion molecules, which are required for the attachment of leukocyte to endothelial cells (rolling lymphocytes) and the interaction between APCs and lymphocytes (Ag presentation) (for review, see Ref. 3). An increase in IMPDH activity has been reported in solid neoplastic cells or in leukemic cells (4, 5), and the administration of IMPDH inhibitors protects patients from developing tumors (6, 7) by a yet undefined mechanism that may involve modulation of cell death (8, 9). Despite >3,000 publications investigating the functional and the molecular effects of MPA on cells, its cytotoxic action remains poorly defined. If activation of caspases is considered as essential to induce the MPA-mediated cell death signal, to date the molecular mechanism responsible for caspase activation upon MPA incubation is unknown (8–10).

Cell death has been divided into three pathways: programmed cell death, also termed apoptosis, autophagic cell death, and necrotic cell death (11). Because numerous markers exist to accurately define the activation status and the intensity of the apoptotic process, this signaling pathway has been extensively studied. Indeed, cleavage of a cysteine protease family-termed caspases (for review see Ref. 12) is an useful marker to easily define whether cells are dying from an apoptotic signal. Although necrosis has long been described as an unanticipated and inappropriate destruction of the cell (13), recent clues challenge this dogma (14, 15).

In the context of allogeneic organ transplant, down-regulation of the immune system is usually reached by using a combination of two immunosuppressors such as azathioprine or MMF associated with cyclosporin A or tacrolimus. Cyclosporin A and tacrolimus are potent inhibitors of the phosphatase calcineurin (protein phosphatase 2B) (16), which prevents the activation of NF-AT an essential step in lymphocyte activation, proliferation, and synthesis of the cytokine IL-2. Azathioprine and its active compound, 6-mercaptopurine, block lymphocyte proliferation by acting on still poorly defined molecular targets that disturb the purine synthesis (17).

In this study we showed that specific inhibition of the IMPDH mediates elimination of lymphocytes, basically through

*Université de Bordeaux-2, Bordeaux, France; †Centre National de la Recherche Scientifique, Unité Mixte de Recherche 5164, Bordeaux, France; ‡Institut Fédératif de Recherche 66, Bordeaux, France; §Centre Hospitalier Universitaire de Bordeaux, Bordeaux, France; ¶Department de Pharmacologie Clinique et Toxicologie, Centre Hospitalier Universitaire de Bordeaux, Bordeaux, France; ‖Institut National de la Santé et de la Recherche Médicale Unité 657, Bordeaux, France; #Centre National de la Recherche Scientifique, Unité Mixte de Recherche 5095, Bordeaux, France

Received for publication April 2, 2008. Accepted for publication October 1, 2008.

The costs of publication of this article were defrayed in part by the payment of page charges. This article must therefore be hereby marked *advertisement* in accordance with 18 U.S.C. Section 1734 solely to indicate this fact.

[1] This work was supported by grants from Association pour la Recherche sur le Cancer (Grant 3798), Fondation de France, Agence Nationale de Recherches (Grant JC07_183182), Ligue Contre le Cancer (Comité de la Dordogne), and Agence de Biomédecine. P.L. is employed by Institut National de la Santé et de la Recherche Médicale. B.C.D. is supported by the Fondation de France (Postdoctoral Fellowship in Leukemia).

[2] B.C.-D. and G.G. share common authorship.

[3] Address correspondence and reprint requests to Dr. Patrick Legembre, Université de Bordeaux, 146 Rue Léo Saignat, 33076 Bordeaux, France. E-mail address: patrick.legembre@inserm.fr

[4] Abbreviations used in this paper: IMPDH, inosine 5′-monophosphate dehydrogenase; CytD, cytochalasin D; FADD, Fas-associated death domain protein; LC3, L chain 3; LtnA, latrunculin A; MMF, mycophenolate mofetil; MNNG, *N*-methyl-*N*′-nitro-*N*′-nitrosoguanidine; MPA, mycophenolic acid; pNA, *p*-nitroanilide; RIP, receptor-interacting protein; SLE, systemic lupus erythematosus; zVAD-fmk, *N*-benzyloxycarbonyl valine-alanine-aspartate-fluoromethylketone.

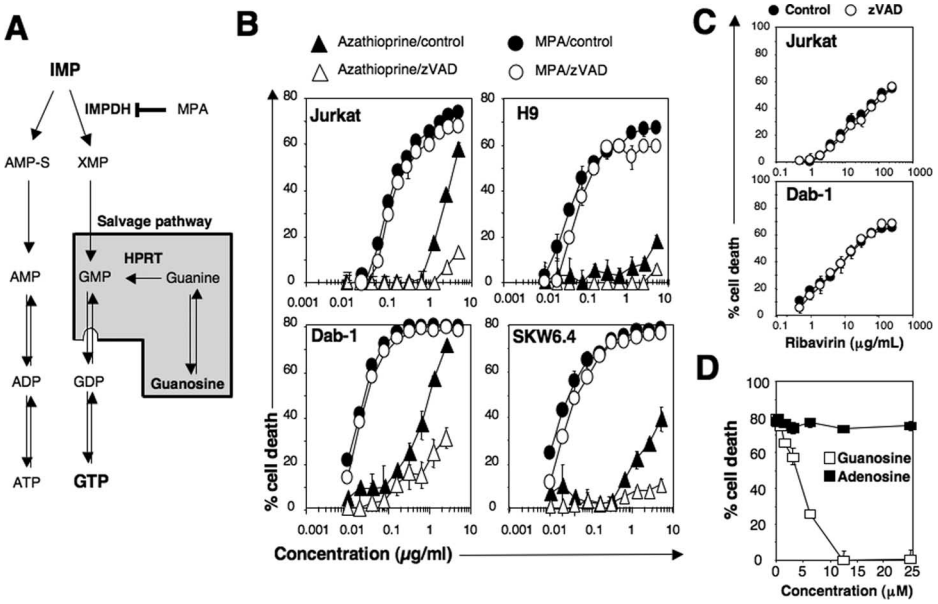

FIGURE 1. MPA induces a caspase-independent cell death signal through inhibition of IMPDH activity. *A*, The de novo synthesis of guanosine tri-phosphate. The salvage pathway is depicted in gray. IMP, Inosine monophosphate; XMP, xanthine monophosphate; HPRT, hypoxanthine-guanine phosphoribosyltransferase. *B*, Azathioprine and MPA-mediated cell death was assessed using a MTT viability assay. The T cell lines (Jurkat, H9) and the B cell lines (SKW6.4, Dab-1) were pretreated with or without caspase inhibitor zVAD-fmk (50 μM) for 30 min and the cells were then stimulated with the indicated dose of azathioprine or MPA for 48 h. *C*, The T cell line Jurkat and the B cell line Dab-1 were preincubated in presence of zVAD-fmk (50 μM) or DMSO (control) for 30 min and the cells were then stimulated with the indicated dose of ribavirin for 48 h. Total cell death was measured by MTT. *D*, The Jurkat T cell line was preincubated for 30 min with the indicated concentration of guanosine or adenosine and then treated with MPA (3 μg/ml) for 48 h. Cell death was measured using the MTT assay. Results shown represent the mean ± SD of three independent experiments.

a novel and atypical necrotic signal that requires actin cytoskeleton polymerization.

Materials and Methods

Cell lines and PBLs

The T cell lines Jurkat, CEM, and H9 and the EBV-transformed B lymphoblastoid cells Dab-1 and SKW6.4 were grown in RPMI 1640 supplemented with 8% FCS. Fas-associated death domain protein (FADD)-deficient Jurkat (I 2.1) and A3 control cells were purchased from American Type Culture Collection. The SVT35 and the receptor-interacting protein (RIP)-deficient Jurkat cells were provided by Dr. B. Seed (Harvard Medical School, Boston, MA). The pEGFP-Bcl-2 plasmid was provided by Dr. R. Youle (National Institutes of Health, Bethesda, MD). The generation of stable clones overexpressing Bcl-2 cells is described elsewhere (18). PBLs from healthy donors were isolated and stimulated as previously described (19).

Cells (5.10^6 cells in 0.3 ml) were electroporated with 10 μg of DNA using a BTM 830 electroporation generator (BTX Instrument Division). Twenty-four hours later, living cells were isolated using the Ficoll separation method.

Reagents

Mycophenolic acid, azathioprine, and DiOC6 were purchased from Sigma-Aldrich. Homemade soluble FasL was generated in the laboratory (20). *N*-benzyloxycarbonyl valine-alanine-aspartate-fluoromethylketone (zVAD-fmk), cytochalasin D, latrunculin A, and *Clostridium difficile* toxin B were purchased from Calbiochem. The plasmids containing the GFP-fused GTPases mutants N17-Cdc42, N17-Rac1, and N19-RhoA were obtained from Dr. P. Fort (Centre de Recherche de Biochimie Macromoléculaire, Montpellier, France). The anti-human caspase-3 mAb was purchased from BD Pharmingen. The anti-human caspase-8 (C-15) mAb was purchased from Axxora. The anti-microtubule-associated protein (MAP) L chain 3 (LC3) mAb was from Affinity Bioreagents, anti-Cdc42 was from BD Biosciences, anti-Rac1 was from Upstate Biotechnology, and anti-RhoA was from Santa Cruz Biotechnology. The anti-β-actin mAb was from Sigma-Aldrich.

Detergent lysis experiments and Western blot analysis

Cells were lysed for 30 min at 4°C in lysis buffer (25 mM HEPES (pH 7.4), 1% Triton X-100, and 150 mM NaCl, supplemented with a mix of protease inhibitors (Sigma-Aldrich)). Protein concentration was determined using the bicinchoninic acid method (Sigma-Aldrich) according to the manufacturer's protocol. Proteins were separated by SDS-PAGE on a 12% gel in reducing conditions and transferred to a nitrocellulose membrane (Amersham Biosciences). The membrane was blocked 1 h with TBST (50 mM Tris, 160 mM NaCl, 0.1% Tween 20 (pH 7.8)) containing 5% dried skimmed milk, and all subsequent steps were performed in this buffer. Specific primary Ab was incubated overnight at 4°C. After intensive washes, the secondary peroxidase-labeled Ab was added for 1 h and the proteins were visualized with the ECL substrate kit (Amersham).

Analysis of caspase activity

Following treatment, 1–2 × 10^6 cells were lysed and incubated with the caspase-8 (Ile-Glu-Thr-Asp (IETD)-*p*-nitroanilide (pNA)) or the caspase-3 (Asp-Glu-Val-Asp(DEVD)-pNA) substrate in a reaction buffer as described in the manufacturer's instructions (Biomol International). The cleavage of caspase substrates (release of the chromophore pNA) was quantified at 405 nm over time using a Titertek Labsystems Multiskan reader.

Cell death assays

Quantification of fragmented DNA (sub-G1 population) was performed as described elsewhere (21). Briefly, treated or untreated cells (0.2 × 10^6) were harvested and incubated for 4 h in 300 μl of buffer containing 0.1% sodium citrate, 0.1% Triton X-100, and 50 μg/ml propidium iodide (Sigma-Aldrich). Cell fluorescence was analyzed by flow cytometry. Cells exhibiting an intensity of fluorescence lower than the G_1-G_0 peak were counted as DNA-fragmented cells.

Total cell death was assessed using MTT assay (metabolic assay), as described previously (22).

To measure cell permeability (damage of the plasma membrane), treated or untreated cells were incubated for 1 h with medium supplemented with 20 μg/ml propidium iodide and immediately analyzed by flow cytometry.

For measurement of mitochondrial potential ($\Delta\psi$m), cells were preincubated with $DiOC_6$ (10 nM) for 15 min and then stimulated with FasL or MPA. Cell fluorescence was measured by flow cytometry.

RhoA, Rac1, and Cdc42 activity assays

GST-PAK-CD and GST-C21 were provided by Dr. J. G. Collard (Netherlands Cancer Institute, Amsterdam, Netherlands). Cloning of the GST-PAK-CD fusion protein containing the Rac and Cdc42 binding region from

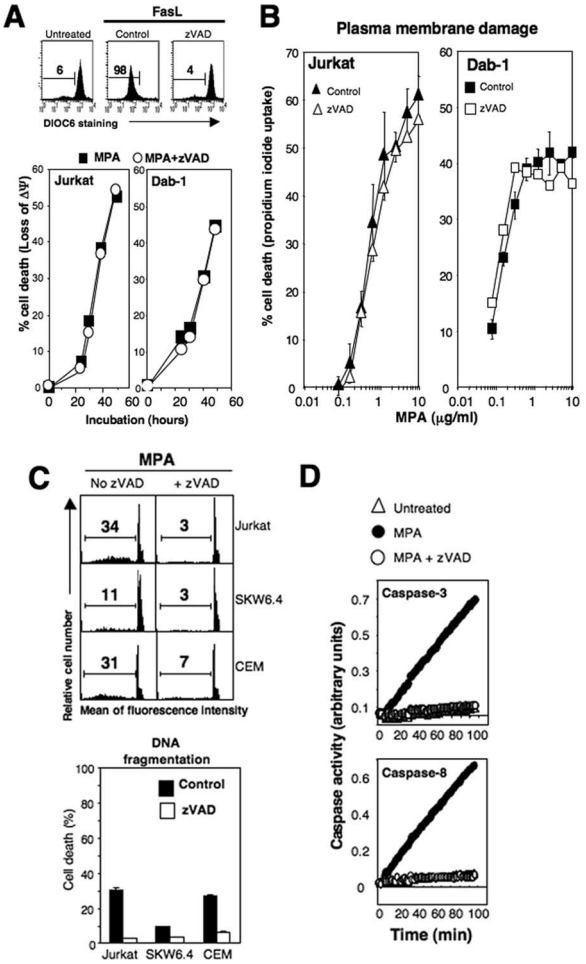

FIGURE 2. MPA-induced cell death is caspase independent. *A*, Mitochondria depolarization was assessed using $DiOC_6$ staining. The T cell line Jurkat and the B cell line Dab-1 were treated with or without zVAD-fmk (zVAD; 50 μM) and next stimulated with MPA (3 μg/ml) for the indicated times. In the *upper panel* are depicted histograms of DiOC6 staining obtained with Jurkat cells preincubated for 30 min in presence of zVAD-fmk (50 μM) or DMSO (control) and then untreated or treated for 6 h with the apoptotic inducer FasL (100 ng/ml). In the lower panel, cells were incubated for 30 min with 50 μM zVAD-fmk or DMSO and DiOC6 fluorescence was analyzed using flow cytometry. The percentage of cells that underwent a loss of mitochondria $\Delta\psi$ was reported. *B*, T (Jurkat) and B (Dab-1) cell lines were treated as described above and then incubated for 1 h with the fluorescent DNA intercalating agent propidium iodide (20 μg/ml). Influx of propidium iodide was analyzed by flow cytometry and the percentage of fluorescent cells was plotted. *C*, Indicated cells were treated with or without zVAD-fmk (50 μM) for 30 min before stimulation with MPA (3 μg/ml) for 48 h. DNA fragmentation (sub-G1 cell population) was determined using flow cytometry analysis as described in *Materials and Methods*. *Lower panel*, The results shown represent the mean ± SD of three independent experiments. *D*, Jurkat cells were preincubated for 30 min with zVAD-fmk (50 μM) or DMSO and then treated or untreated with MPA (3 μg/ml) for 48 h. Cells were lysed and caspase-8 (initiator) or caspase-3 (executioner) activities were quantified over time by adding Ile-Glu-Thr-Asp (IETD)-pNA or Asp-Glu-Val-Asp (DEVD)-pNA, respectively. Data are representative of five independently performed experiments.

human PAK1B, has previously been described (23). GST-C21 has been described (24) and contains the Rho binding domain, from the Rho effector protein Rhotekin. Recombinant proteins were prepared as described (23).

GTPase activity assays were conducted as previously described (23). In brief, cells were treated or untreated for the indicated times and lysed for 30 min in a lysis buffer (50 mM Tris, 150 mM NaCl, 0.1% SDS, 0.5% sodium deoxycholate, and 1% Triton X-100, supplemented with mixtures of protease and phosphatase inhibitors) effective for solubilizing the plasma membrane-distributed small GTPases (23). The cell lysates were next incubated for 2 h with GST-PAK-CD or GST-C21 bound to glutathione-coupled Sepharose beads. Beads were washed in lysis buffer and resuspended in Laemmli sample buffer. The amount of bound Cdc42, Rac1, or RhoA molecules was analyzed by Western blotting.

Flow cytometry

Cells were washed in PBS with 1% (w/v) BSA, and fluorescence was immediately analyzed using a FACScalibur flow cytometer (BD Bioscience).

Immunofluorescence and imaging

Cells were let to adhere for 5 min at room temperature to poly-L-lysine-coated slides (ESCO, VWR). Cells were fixed in PBS with 2% PFA for 30 min, washed, and then treated for 15 min with PBS containing 5% FCS to quench aldehyde groups. Cells were permeabilized for 5 min at 4°C using PBS and 0.1% Triton X-100 and stained with tetramethylrhodamine isothiocyanate-linked phalloidin (Sigma-Aldrich) (1 μg/ml) for 30 min at 4°C. Slides were washed, dried, and mounted with fluorescent mounting medium (DakoCytomation). Images were analyzed with a confocal microscope (Leica SP5) with a ×63 objective.

Electronic microscopy

Stimulated cells (10^7) were fixed for 1 h at 4°C in 1.5% glutaraldehyde (0.1M phosphate buffer), postfixed in 1% osmium tetroxide for 1 h at 4°C, dehydrated in ethanol, and embedded into a Epon resin mixture. Sections were stained using uranyl acetate and lead citrate and sections were analyzed using a FEI Tecnai 12 BioTwin transmission electron microscope. Pictures were acquired with a Gatan Orius wide-angle camera (11 megapixels).

Results

MPA induces a caspase-independent cell death signal

T and B leukemia cell lines were incubated with therapeutic concentrations of azathioprine, MPA, cyclosporin A, or tacrolimus. Whereas cells were efficiently eliminated upon MPA and azathioprine treatments (except for the azathioprine-resistant T lymphoma cell line H9; Fig. 1*B*), cyclosporin A and tacrolimus either exerted a faint cytotoxic effect or were devoid of one (data not shown). As caspase activity is the landmark of the apoptotic signal, we next determined the role of these proteases in the MPA and azathioprine-mediated cell death signals. Strikingly, whereas preincubation of cells with the pan-caspase inhibitor zVAD-fmk prevented cell death mediated by azathioprine treatment (Fig. 1*B*), it was inoperative on the cytotoxic effect of MPA (Fig. 1*B*). Identical results were obtained using the executioner caspase inhibitor DEVD-chloromethyl ketone (data not shown). To confirm that this caspase-independent signal relied on the inhibition of IMPDH, we treated the cells with a competitive inhibitor of IMPDH called ribavirin (25). Identically to MPA, ribavirin induced a caspase-independent cell death signal in T or B cell lines (Fig. 1*C*). These findings indicated that in contrast to other immunosuppressive agents, MPA generated a caspase-independent cell death in T and B cell lines through the inhibition of IMPDH.

Inhibition of IMPDH leads to a decrease of the intracellular pool of GTP (26), which can be counterbalanced by the addition of exogenous guanosine (Fig. 1*A*, see "Salvage pathway"). To demonstrate that MPA-mediated cell death was specifically due to the abrogation of IMPDH activity, rescue of cells by the addition of guanosine was analyzed. Adenosine acts on the ATP pool and was used as a control. Although adenosine did not modify the MPA-mediated cell death, guanosine abrogated the cytotoxic effect of MPA (Fig. 1*D*) indicating that cell death was exclusively mediated through the inhibition of IMPDH.

MPA kills cells mainly through a caspase-independent cell death

It was conceivable that MPA-mediated depletion of GTP could account for a general decrease of the metabolic activity in living

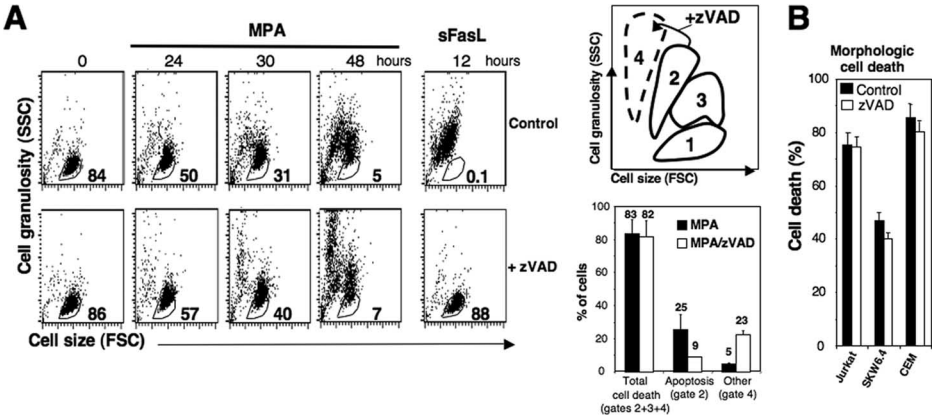

FIGURE 3. Morphological analysis of MPA-mediated cell death. *A*, Jurkat cell line was incubated with MPA and the cell morphology was examined using flow cytometric parameters, forward scatter (FSC; cell size), and side scatter (SSC; granularity). Cells were treated or untreated with the caspase inhibitor zVAD-fmk (50 μM) and then stimulated with MPA (3 μg/ml) or soluble FasL (sFasL) (100 ng/ml) for indicated times. Numbers indicate the percentage of living cells contained in the gate. Jurkat cells preincubated in the presence or absence of zVAD-fmk (50 μM) were treated for 48 h with 5 μg/ml MPA and the histogram depicts the percentage of cells encompassed into gate 2, gate 4, or total cell death. *B*, Indicated T and B cell lines were treated or untreated with zVAD-fmk (50 μM) and then incubated for 48 h with MPA (3 μg/ml). The percentage of cells comprised in gate 3 was displayed. Results shown are representative of at least three independent experiments.

cells and that the MTT assay measuring the mitochondrial and cytoplasmic dehydrogenase activities was not a faithful indicator of cell death. To rule out this possibility, MPA-mediated cell death was assessed using several methods quantifying the loss of mitochondrial potential ($\Delta\psi$m), DNA fragmentation (apoptosis), morphological changes, and plasma membrane damage (propidium iodide influx). Engagement of the apoptotic receptor Fas (APO1/CD95) led to complete mitochondria depolarization, and inhibition of the caspase activity reverted the loss of $\Delta\psi$m (Fig. 2*A*, *upper panel*). In contrast, MPA treatment induced the depolarization of the mitochondria independently of the caspase activity (Fig. 2*A*, *lower panel*). MPA also induced damages of the plasma membrane that were not prevented by the use of zVAD-fmk (Fig. 2*B*). Surprisingly, a small part of the MPA-treated cells harbored fragmented DNA, a hallmark of apoptosis, and these cells were protected from death by zVAD-fmk preincubation (Fig. 2*C*). It was confirmed that some cells were dying through an apoptotic signal, because caspase-8 and caspase-3 activities were detected in the whole lysates of MPA-treated cells (Fig. 2*D*). These findings pointed out that upon MPA treatment, a major part of the cells died through a caspase-independent signal while a minor part of the cells were eliminated by a caspase-dependent apoptotic signal.

Inhibition of caspase activity did not impinge on total MPA-mediated cell death (Figs. 1*B* and 2, *A* and *B*). One possibility to explain this discrepancy was that the caspase inhibitor zVAD-fmk did not fully inhibit the catalytic activity of these proteases. Using caspase activity assays, we ruled out this possibility because the pan-caspase inhibitor totally abrogated the caspase activities in MPA-treated cells (Fig. 2*D*).

Caspase-independent cell death exhibits necrotic features

Flow cytometric parameters, cell size (forward scatter) and granule content of the cells (side scatter), allowed us to define a window corresponding to the living cells (untreated cells; see black gate in Fig. 3*A*). Based on the cell population that died upon treatment with the apoptotic inducer FasL, a second window was defined corresponding to the apoptotic morphology (gate 2 in the pictogram, Fig. 3*A*). This cell population was a minority (between 10 and 30%) and died through a caspase-dependent signal because zVAD-fmk preincubation dramatically decreased the percentage of the cells present within this gate (see histogram, Fig. 3*A*). MPA treatment revealed a third population that appeared rapidly (24 h), comprised a majority of cells, and harbored a size similar to that of living cells but contained more granules (gate 3). Cells encompassed within the gate 3 were insensitive to the zVAD-fmk pretreatment (see Fig. 3, *A* and *B*). Strikingly, the decrease in the number of apoptotic cells due to caspase inhibition was counterbalanced by the appearance of a fourth population corresponding to small and highly granular cells (gate 4) (see histogram in Fig. 3*A*).

To identify the types of cell death induced upon MPA treatment, we used transmission electron microscopy. The T leukemia cell line Jurkat harbored a large nucleus containing one or more nucleoli, and the cytoplasm was homogeneous and devoid of any vacuoles (Fig. 4*A*). FasL stimulation led to a drastic modification of the cellular shape with the cytoplasmic accumulation of vacuoles and the condensation of chromatin around the nuclear periphery (Fig. 4*A*), a morphology typical of apoptotic cells (27). In contrast, following treatment with MPA a majority of cells (70 to 90%) displayed a loss of their plasma membrane integrity, mitochondria swelling, and, more strikingly, no trace of chromatin condensation (Fig. 4*A*). These morphological features are hallmarks of cells dying through a necrotic process (27). Ten to 30% of the cells treated with MPA displayed apoptotic features (data not shown) and the zVAD-fmk pretreatment eliminated this minor population, which was replaced by small sized cells exhibiting a cytoplasm containing numerous granules (Figs. 4*B* and *3A*). Using higher magnification, these cells displayed accumulation of double-membrane vacuoles containing degraded organelles (see filled arrowheads; Fig. 4*B*), a hallmark of autophagic cells. Two forms of microtubule-associated protein 1 LC3 exist, a cytosolic LC3-I and an autophagosome membrane-bound LC3-II considered as a marker of the autophagic process (28). The autophagic population was confirmed in B and T cell lines, because the amount of LC3-II significantly increased when cells were preincubated with zVAD-fmk and treated with MPA (Fig. 4*C*).

In summary, MPA kills T and B lymphoma cell lines by inducing a necrotic morphology. For unknown reasons, a minority of the cells did not undergo the necrotic process but instead were eliminated via a caspase-dependent apoptotic signal. Upon inhibition of caspases, the cells protected from apoptosis underwent death through an autophagic process (see Figs. 3*A* and 4, *B* and *C*).

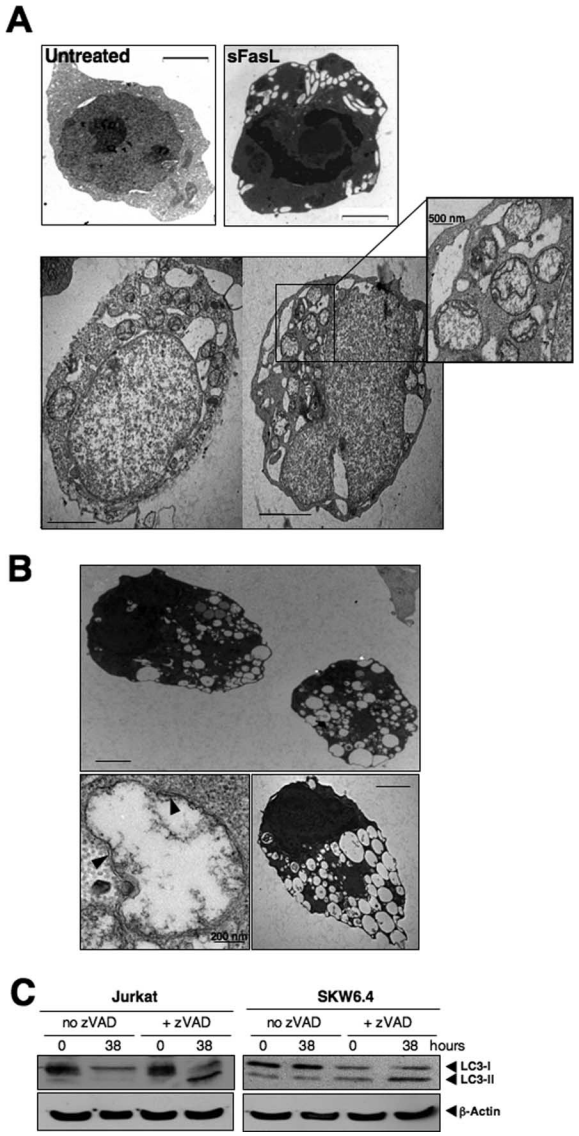

FIGURE 4. Transmission electron microscopy analysis of MPA-mediated cell death. *A* and *B*, Bars = 2 μm, except where indicated. *A*, Electron micrographs of Jurkat cells incubated with or without soluble FasL (sFasL; 100 ng/ml) for 4 h (apoptosis). Jurkat cells were pretreated with or without caspase inhibitor zVAD-fmk (50 μM) and then stimulated with MPA (3 μg/ml) for 44 h. The *inset* depicts a zoom of swelling mitochondria. In the *inset*, higher magnification was used to analyze morphology of the mitochondria. *B*, Jurkat cells were preincubated with zVAD-fmk (50 μM) for 30 min and then treated for 44 h with 3 μg/ml MPA. Electron microscopic analysis revealed that a minor part of the cells (10–30%) harbored accumulation of double-membrane autophagic vacuoles (see black arrowheads). Pictures are representative of at least five independent experiments. *C*, The T leukemic cell line Jurkat and the B lymphoma cell line SKW6.4 were treated or untreated with zVAD-fmk (zVAD; 50 μM) and then incubated for the indicated times with MPA (3 μg/ml). Cells were lysed and 100 μg of protein was separated by electrophoresis in a 15% SDS-polyacrylamide gel. Soluble (LC3-I), membrane-bound LC3 (LC3-II) and β-actin (loading control) were analyzed by Western blotting.

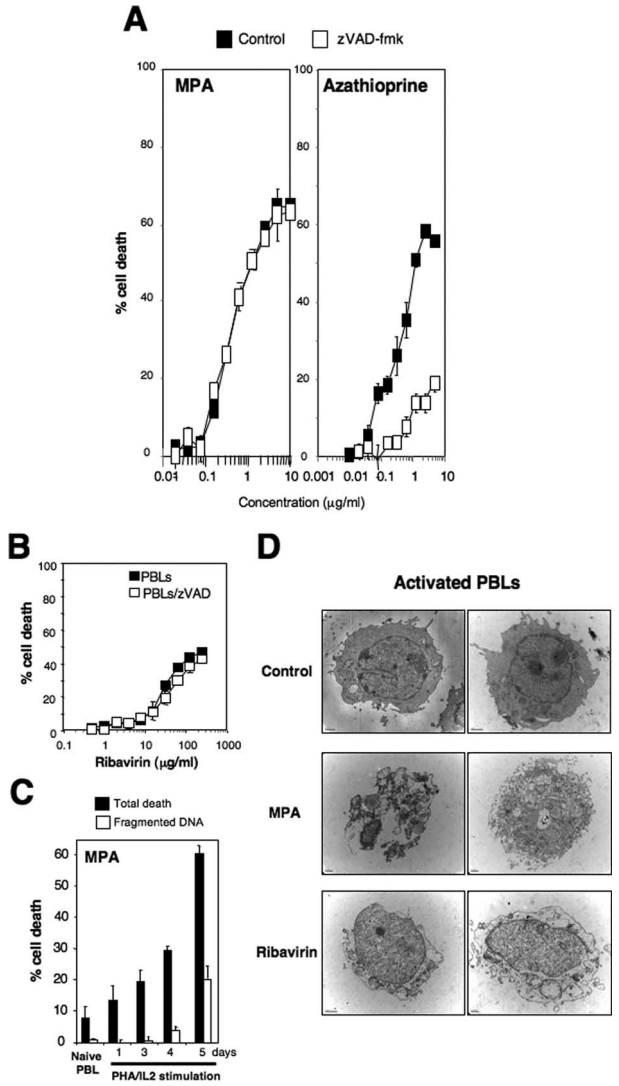

FIGURE 5. Activated PBLs are killed by necrosis upon MPA addition. *A*, Activated PBLs (PHA/IL-2) were treated with or without zVAD-fmk (50 μM) for 30 min and then incubated with MPA or azathioprine for 48 h. Total cell death was measured using a MTT viability assay. *B*, Activated PBLs (PHA/IL-2) were preincubated with zVAD-fmk (zVAD; 50 μM) or DMSO (control) for 30 min, and then treated with ribavirin for 48 h. Cell death was measured using a MTT viability assay. *C*, Naive (unstimulated) or activated PBLs were harvested at different times of activation and incubated with MPA (3 μg/ml) for 48 h. Cell death was determined during PBL activation using MTT viability (total cell death) and DNA fragmentation assays (apoptosis). Results shown represent the mean ± SD of three independent experiments. *D*, Transmission electron micrographs of activated PBLs incubated with DMSO (control), MPA (10 μg/ml), or ribavirin (100 μg/ml) for 40 h. Pictures are representative of at least three independent experiments.

Activated T lymphocytes are killed through a necrotic signal

To determine whether MPA induced a necrotic signal in primary T lymphocytes, PBLs were harvested from healthy donors, activated, and then incubated with MPA (Fig. 5*A*). Activated lymphocytes were efficiently killed by MPA or ribavirin and both induced a cell death signal independent of the caspase activity (Fig. 5, *A* and *B*). In contrast, azathioprine eliminated the PBLs through a caspase-dependent cell death signal (Fig. 5*A*). Analysis of the DNA fragmentation revealed that similar to data obtained with the cell lines, less than one-third of the MPA-killed T lymphocytes underwent apoptosis (Fig. 5*C*). It was noteworthy that naive PBLs were refractory to MPA-mediated cell death, whereas the activation process of T lymphocytes led to the sensitization of the cells to the MPA-mediated necrotic signal (Fig. 5*C*). Cell morphology analysis using transmission electron microscopy confirmed that inhibition of IMPDH either using MPA or ribavirin triggered necrosis of the activated PBLs (Fig. 5*D*).

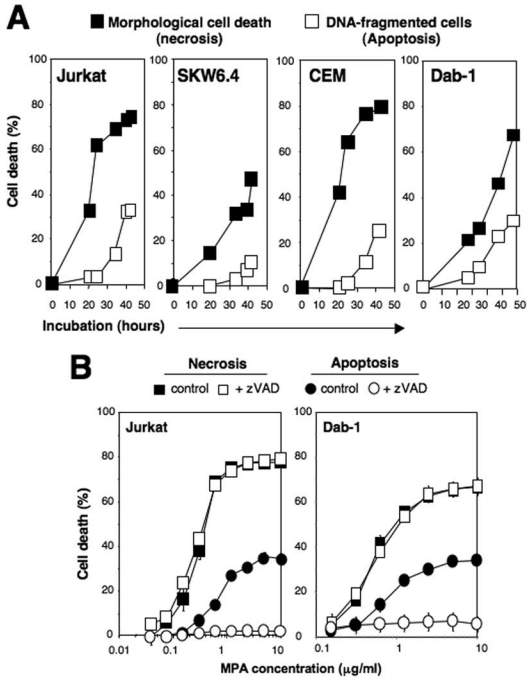

FIGURE 6. The necrotic signal requires short exposure with MPA and a low dose of MPA. *A*, A kinetic analysis was performed with a high concentration of MPA (3 μg/ml) on different T and B cell lines. Cell death was quantified using morphological (necrotic) or DNA fragmentation (apoptotic cell death) assays. *B*, Jurkat and Dab-1 cell lines were preincubated with or without 50 μM zVAD-fmk (zVAD) for 30 min and then treated for 48 h with the indicated concentration of MPA. Necrotic (morphology) and apoptotic (sub-G1 population) cells were quantified.

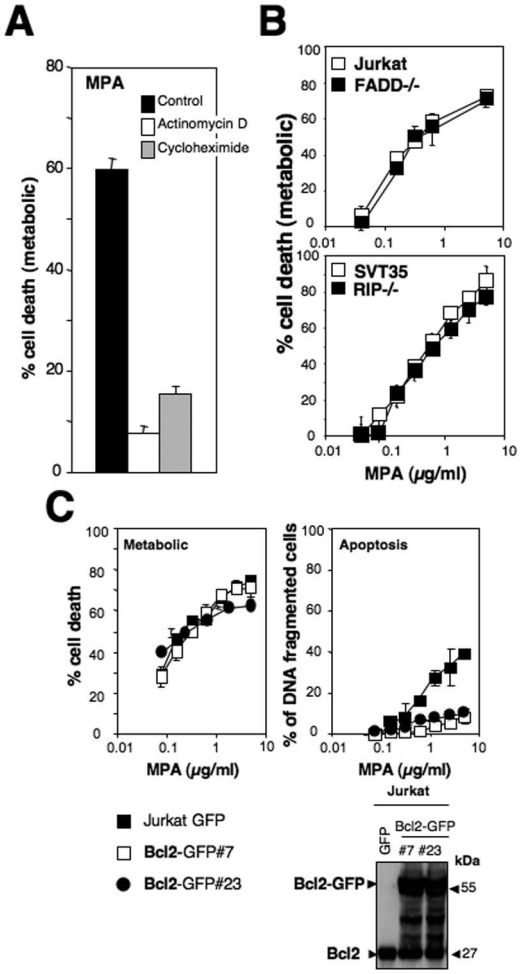

FIGURE 7. The necrotic signal does not rely on FADD or RIP expressions but requires protein synthesis. *A*, The B-lymphoblastoid Dab-1 cell line was preincubated for 1 h with actinomycin D (0.5 μg/ml) or cycloheximide (1 μg/ml) and then treated with MPA (3 μg/ml) for 24 h. Cell death was quantified using the MTT assay. *B*, Parental cells and FADD-deficient or RIP-deficient Jurkat cells were stimulated with MPA for 48 h. Cell death was assessed by MTT. *C*, Jurkat cells expressing GFP or the chimera protein GFP-Bcl2 were treated with or without MPA for 48 h and total dead cells (metabolic assay MTT) or apoptotic cells (sub-G1 cell population) were assessed. Expression of GFP-Bcl2 in each clone was estimated by immunoblotting. The indicated cells were lysed and 50 μg of protein was subjected to SDS-PAGE. Endogenous and GFP-fused Bcl2 were revealed using an anti-Bcl2 mAb. Results represent the mean ± SD of three independent experiments.

MPA mediates a rapid and efficient necrotic signal

Necrosis is currently considered to be an uncontrolled mechanism that is observed when high doses of cytotoxic agents are used and/or the apoptosis process is abrogated (14). To determine whether the MPA-mediated necrotic signal occurred because the apoptotic pathway was altered, we analyzed the kinetics of necrotic and apoptotic cell death by measuring simultaneously DNA fragmentation (apoptosis) and morphological cell death (necrosis) as described above. The appearance of apoptotic cells was dramatically delayed compared with that of the necrotic cells (Fig. 6*A*). Indeed, whereas 10–20 h of incubation with MPA were sufficient to eliminate 20% of the cells via a necrotic process, the incubation had to be prolonged from 35 to 55 h to reach a similar percentage of DNA-fragmented cells (Fig. 6*A*). Because necrosis has been reported to occur when elevated concentrations of agent are used (14), we conducted a dose-effect analysis of MPA on B and T cell lines. We observed that whereas low doses of MPA between 0.1 and 0.4 μg/ml were sufficient to reach 20 to 25% of necrotic cells insensitive to zVAD-fmk pretreatment (morphologic cell death in Fig. 6*B*), 1 μg/ml MPA was necessary to quantify the same amount of caspase-dependent apoptotic cells (DNA fragmented cells in Fig. 6*B*). In conclusion, low doses of MPA induced a rapid and efficient necrotic cell death signal that took place before the induction of a delayed apoptotic signal requiring elevated concentrations of MPA.

MPA-mediated necrotic signal is independent of FADD and RIP

It has been reported that high doses of FasL induce a necrotic pathway that is amplified by both translation and transcription inhibitors (14). Hence, we examined the effect of de novo translation or transcription inhibition on the MPA-mediated necrotic signal. Strikingly, cycloheximide or actinomycin D incubations dramatically inhibited the MPA-mediated necrotic signal (Fig. 7*A*). Because the adaptor protein FADD and the serine-threonine kinase RIP have been reported as being essential for the transmission of a necrotic signal in T lymphocytes (14), we next examined the putative role of these proteins in the MPA signal. The RIP- and the FADD-deficient Jurkat T cell lines and their respective parental cell lines were incubated with MPA for 48 h and metabolic cell death was measured (Fig. 7*B*). The absence of FADD or RIP did not alter the MPA cell death signal (Fig. 7*B*). Recently, an atypical necrotic signal has been characterized in cells treated with the DNA-alkylating agent *N*-methyl-*N*′-nitro-*N*′-nitrosoguanidine (MNNG). This signal was prevented by the overexpression of the antiapoptotic factor Bcl2 (29). To determine the effect of Bcl2 upon the MPA-mediated necrotic signal, we overexpressed this

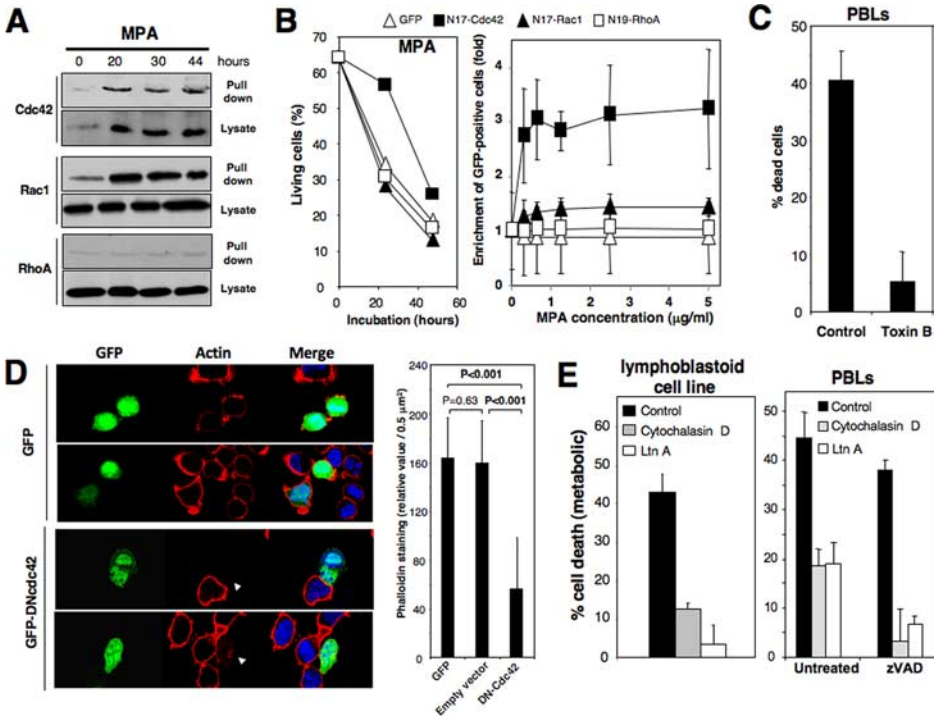

FIGURE 8. Cdc42 activity and polymerized actin are essential for transmission of the necrotic signal. *A*, Jurkat cells were stimulated with MPA (3 μg/ml) for the indicated times and cells were lysed. Proteins (100 μg per lane) were separated by SDS-PAGE. Expression of RhoA, Cdc42, and Rac-1 were detected by immunoblotting (lysate). To quantify the activity of RhoA, Cdc42, and Rac1, pull-down assays were conducted as described in *Materials and Methods*. *B*, Jurkat cells were transiently transfected with expression vectors encoding the dominant negative constructs N17-Cdc42-GFP, N17-Rac1-GFP, and N19-RhoA-GFP or GFP alone. *Left panel*, Transfected cells were stimulated with MPA (3 μg/ml) and the viable cells were quantified using morphology analysis (flow cytometry). *Right panel*, the transfected cells were stimulated with MPA and the ratio of GFP-positive cells to living cells was quantified using flow cytometry. *C*, Activated PBLs (1 day with PHA followed by 5 days with IL-2) were preincubated with *C. difficile* toxin B (500 nM) for 1 h and then treated for 48 h with 1 μg/ml MPA. *D*, The T cell line H9 was transfected with pEGFP plasmid or the pEGFP-N17-Cdc42. Living cells were isolated using the Ficoll method and polymerized actin was stained using tetramethylrhodamine isothiocyanate-linked phalloidin. Images were acquired and processed with a confocal microscope (Leica SP5) using a $\times$63 objective. White arrowheads indicate the barely detectable phalloidin staining in the dominant negative Cdc42 (N17-Cdc42)-expressing cells. The relative amount of polymerized actin was assessed by densitometry (ImageJ analysis) in quantifying the intensity of phalloidin fluorescence (area of 0.5 μm^2) under the plasma membrane of indicated cells. Independent counts (46 counts) were performed and the mean of fluorescence ($\pm$SD) was depicted. Statistical analysis was conducted using a Mann-Whitney test. *E,* The B lymphoblastoid cell line Dab-1 and activated PBLs were preincubated with cytochalasin D (5 μM, 30 min), latrunculin A (5 μM, 30 min), or DMSO (control) and stimulated with MPA (3 μg/ml for Dab-1 and 1 μg/ml for activated PBLs) for 48 h. PBLs were preincubated with zVAD-fmk (zVAD; 50 μM) or DMSO (untreated). Results represent the mean $\pm$ SD of three independent experiments.

antiapoptotic factor in the Jurkat T cell line (stable clones expressing the chimera GFP-Bcl2 are depicted in Fig. 7*C*). Bcl2 overexpression efficiently rescued cells dying through the apoptotic process, whereas it did not impinge on the total cell death (Fig. 7*C*). Altogether, these findings indicated that MPA triggered a RIP-, FADD-, and Bcl2-independent necrotic signal distinct from the ones induced by both MNNG (29) and FasL (14).

The necrotic signal requires Cdc42 activation and polymerized actin

Recently, it has been shown that adenoviruses are able to activate members of the Rho-GTPases and thus induce an atypical cell death in cancer cells (30). Therefore, the expression level and the activity status of the principal Rho GTPases were analyzed upon incubation with MPA. Whereas the protein expression of RhoA and Rac1 remained constant during the MPA incubation (Fig. 8*A*), the MPA addition induced an increase of the Cdc42 protein level between 20 and 30 h (Fig. 8*A*). Using Rac1/Cdc42 and RhoA-specific effectors fused to GST in a pull-down assay (23), we quantified the amount of active GTPases during MPA treatment. Despite large amounts of RhoA in the cells, its active form was barely detectable and its activation level remained weak during MPA treatment (Fig. 8*A*). In contrast, Rac1 and Cdc42 were activated after 20 h of contact with MPA and remained active up to 44 h (Fig. 8*A*). Next, Jurkat and Dab-1 cell lines were transfected with dominant negative variants of the different Rho GTPases fused to the fluorescent protein GFP. Transiently transfected cells (20–30% of GFP-containing cells) were incubated with MPA and the percentage of living cells and the enrichment of GFP-expressing cells in this population were quantified (Fig. 8*B*). Strikingly, the ectopic expression of a dominant negative Cdc42 (N17-Cdc42) significantly protected the cells from MPA-mediated cell death (Fig. 8*B*, *left panel*). Furthermore, the ratio of green cells (GFP-positive cells) expressing the mutated Cdc42 (N17-Cdc42) was dramatically increased inside the living cell population (Fig. 8*B*). In contrast, transfection of GFP alone or RhoA and Rac1 dominant negative constructs neither modified the percentage of living cells (Fig. 8*B*, *left panel*) nor the ratio of GFP-positive cells upon MPA incubation (Fig. 8*B*, *right panel*). The B lymphoblastoid cell line Dab-1 was similarly protected from the MPA necrotic signal upon N17-cdc42 expression (data not shown). *C. difficile* toxin B (toxin B) inhibits the biological activity of the Rho-GTPases (31). To validate that the activity of Rho-GTPases was essential to transmit necrosis in activated PBLs, we

incubated lymphocytes with toxin B. As can be observed in Fig. 8*C*, toxin B dramatically altered the MPA-mediated necrotic signal. These data indicated that Cdc42 was involved in the transmission of the necrotic signal.

Because Cdc42 is a key regulator of essential cellular functions such as cytoskeletal dynamics (32), we next evaluated whether the effect of Cdc42 on necrosis could be associated with its action on the actin cytoskeleton. A polymerized form of actin (actin-F) was labeled with the cyclic peptide phalloidin (33). As observed by confocal microscopy, T cells exhibited polymerized actin around the periphery of the cell (Fig. 8*D*). Whereas GFP alone did not modify the pattern of the polymerized actin network, the dominant negative Cdc42 significantly impaired the phalloidin labeling (see white arrowheads and densitometry analysis in Fig. 8*D*). To determine whether the necrotic signal was dependent on the polymerized actin network, we next tested the effect of two inhibitors of actin polymerization (latrunculin A (LtnA) and cytochalasin D (CytD)) on MPA-mediated cell death. Using noncytotoxic doses of LtnA and CytD, we showed that inhibition of actin polymerization dramatically abrogated the MPA-mediated cell death (Fig. 8*E*). Although these drugs displayed a significant effect (60% of inhibition) to prevent MPA-mediated necrosis in activated PBLs (Fig. 8*E*), their actions were weaker than that observed on the B cell line. Nevertheless, when caspase activity was inhibited, both LtnA and CytD totally abrogated the cell death signal in activated PBLs (Fig. 8*E*). Taken together these data showed that the remodeling of polymerized actin played an essential function in the transmission of the caspase-independent signal induced by MPA.

Discussion

Using different approaches, we demonstrated that the widely used immunosuppressive agent MPA triggers a potent and rapid necrotic signal. This necrotic signal was uniquely triggered upon MPA treatment, because other currently used immunosuppressive agents are either poorly cytotoxic (cyclosporin A, tacrolimus) or induce an apoptotic signal abrogated by zVAD-fmk (azathioprine). Using T and B cell lines or activated PBLs, we showed that MPA induces apoptosis (caspase-dependent signal) of a minor part of the cell population. It is conceivable that this marginal effect of the immunosuppressive agent could have misled authors who previously reported that the MPA cytotoxic effect was mediated through an apoptotic signal (9, 10, 34). Inhibition of the caspase activity was not sufficient to rescue the small cell population dying through apoptosis, because blockade of caspase activity led to the induction of autophagic cell death. We could argue that caspase activation and DNA fragmentation occur secondarily to the necrotic events and, hence, all of the cells in fact undergo necrosis. Nevertheless, this hypothesis is ruled out because the irreversible features observed in the necrotic cells (swelled mitochondria and plasma membrane breakdown) were not detected anymore in the few cells exhibiting an apoptotic morphology (transmission electron microscopy analysis). To date, why a minor part of the cell population does not respond to the MPA-mediated necrotic signal but rather is eliminated through an apoptotic process remains an open question. The Rho-GTPase Cdc42 is essential in shaping the actin cytoskeleton (35, 36) and, similarly to dominant negative Cdc42, pharmacological agents disturbing actin polymerization prevent the MPA-mediated necrotic signal. For the first time, we demonstrated that inhibition of the IMPDH activity generates cellular stress that leads to a novel and atypical necrotic signal requiring the Cdc42 activity.

The disclosed necrotic signal is not superimposable with the Fas-mediated necrotic signal identified by Tschopp and colleagues because MPA does not rely on the presence of FADD or RIP to trigger cell death (14). Sperandio et al. (37) reported a cell death termed paraptosis, the morphological and molecular features of which resemble the one described here. The paraptosis pathway relies on de novo protein synthesis and mRNA transcription, and the overexpression of Bcl-2 family antiapoptotic members (Bcl-x_L or Bcl-2) or the inhibition of caspase activity is unable to prevent cell death mediated by the insulin-like growth factor I receptor. Identically as in paraptosis, Bcl-2 overexpression was ineffective in inhibiting the MPA-mediated necrotic pathway, although it abrogated the apoptotic signal as quantified using a DNA fragmentation assay. However, whereas ERK and JNK-1 play a pivotal role in the paraptotic signaling pathway (15), activation of these MAPKs were not detected upon MPA treatment and, besides, specific JNK inhibitors were inefficient at preventing cell death triggered by MPA incubation (data not shown). Recently Moubarak and colleagues demonstrated that the DNA-alkylating agent MNNG triggered a necrotic signaling pathway implicating the molecular ordering of PARP-1 (poly(ADP-ribose)-polymerase-1), calpain, Bax, and AIF (apoptosis-inducing factor) (29). The authors observed a partial condensation of the chromatin associated with the cleavage of DNA in fragments of large scale (~50 kbp of length) (29). The MNNG signal was abrogated by Bcl2 overexpression. In contrast to MNNG, the MPA-mediated necrotic signal did not display any trace of chromatin condensation or DNA cleavage; in addition, Bcl2 overexpression did not impinge on the necrotic signal. It is noteworthy that PARP-1, the activity of which is essential to trigger necrosis upon MNNG treatment, was found cleaved and inhibited by the MPA addition to the cell culture (data not shown). In conclusion, in this article we characterized a new and atypical necrotic signal that does not share common signaling hubs with necrotic signals transmitted by high amount of FasL (14) or MNNG (29) or by stimulation of the insulin-like growth factor I receptor (37). Taken together, these findings support the premise that, as is the case for the extensively studied apoptotic signals, necrotic cell death depends on the transmission of different and unrelated genetically controlled process.

Resistance to apoptosis improves the genetic instability of the cell (e.g., DNA-damage foci, aneuploidy, supernumerary centrosome) (38) and is an essential step in tumorigenesis (39) allowing the cell to escape from immunosurveillance (40). High incidence of lymphomas and atypical malignancies are a hallmark of renal transplant recipients (41). Recently, MMF treatment has been shown to decrease the risk of incidence of malignancy as compared with a non-MMF treated cohort of patients, and the incidence of lymphomas was lower in the MMF-exposed group vs the MMF-unexposed group (0.53 vs 0.95%) (42). Because, in contrast to other immunosuppressive agents, MPA incubation drives a potent necrotic signal and the IMPDH-inhibitor is also able to trigger apoptosis or autophagy depending on the functionality of the caspases, MPA-mediated cell death could be an attractive explanation for the lower occurrence of cancer observed in the renal transplanted patient compared with patients treated with azathioprine.

The necrotic signal induced by MPA may also explain why this agent is efficient for treating autoimmune diseases such as systemic lupus erythematosus (SLE). Indeed, it has been reported that deficient phagocytic activity and accumulation of apoptotic bodies could favor the progression of SLE (43). Because MPA mainly eliminated Ag-stimulated cells (not naive cells) through necrosis, we could conceive that the down-modulation of the immune activity associated with an identical or decreased amount of apoptotic bodies may account for the efficiency of MPA in treating SLE (44).

Acknowledgments

We thank Lacomme Sabrina (Pôle Microscopie Electronique de Bordeaux-2) and Senant Nathalie (Cytométrie IFR66) for technical assistance. We thank Dr. Robinson Philip (Laboratoire de Pharmacologie, Université de Bordeaux 2, Bordeaux, France) for critical reading of the manuscript.

Disclosures

The authors have no financial conflict of interest.

References

1. Nankivell, B. J., M. D. Wavamunno, R. J. Borrows, M. Vitalone, C. L. Fung, R. D. Allen, J. R. Chapman, and P. J. O'Connell. 2007. Mycophenolate mofetil is associated with altered expression of chronic renal transplant histology. *Am. J. Transplant.* 7: 366–376.
2. Sollinger, H. W. 1995. Mycophenolate mofetil for the prevention of acute rejection in primary cadaveric renal allograft recipients: U.S. Renal Transplant Mycophenolate Mofetil Study Group. *Transplantation* 60: 225–232.
3. Allison, A. C., and E. M. Eugui. 2000. Mycophenolate mofetil and its mechanisms of action. *Immunopharmacology* 47: 85–118.
4. Collart, F. R., C. B. Chubb, B. L. Mirkin, and E. Huberman. 1992. Increased inosine-5′-phosphate dehydrogenase gene expression in solid tumor tissues and tumor cell lines. *Cancer Res.* 52: 5826–5828.
5. Jackson, R. C., G. Weber, and H. P. Morris. 1975. IMP dehydrogenase, an enzyme linked with proliferation and malignancy. *Nature* 256: 331–333.
6. Tressler, R. J., L. J. Garvin, and D. L. Slate. 1994. Anti-tumor activity of mycophenolate mofetil against human and mouse tumors in vivo. *Int. J. Cancer* 57: 568–573.
7. Tricot, G. J., H. N. Jayaram, E. Lapis, Y. Natsumeda, C. R. Nichols, P. Kneebone, N. Heerema, G. Weber, and R. Hoffman. 1989. Biochemically directed therapy of leukemia with tiazofurin, a selective blocker of inosine 5′-phosphate dehydrogenase activity. *Cancer Res.* 49: 3696–3701.
8. Kim, J. Y., S. Y. Yoon, J. Park, and Y. S. Kim. 2006. Mycophenolic acid induces islet apoptosis by regulating mitogen-activated protein kinase activation. *Transplant. Proc.* 38: 3277–3279.
9. Takebe, N., X. Cheng, T. E. Fandy, R. K. Srivastava, S. Wu, S. Shankar, K. Bauer, J. Shaughnessy, and G. Tricot. 2006. IMP dehydrogenase inhibitor mycophenolate mofetil induces caspase-dependent apoptosis and cell cycle inhibition in multiple myeloma cells. *Mol. Cancer Ther.* 5: 457–466.
10. Gu, J. J., L. Santiago, and B. S. Mitchell. 2005. Synergy between imatinib and mycophenolic acid in inducing apoptosis in cell lines expressing Bcr-Abl. *Blood* 105: 3270–3277.
11. Galluzzi, L., M. C. Maiuri, I. Vitale, H. Zischka, M. Castedo, L. Zitvogel, and G. Kroemer. 2007. Cell death modalities: classification and pathophysiological implications. *Cell Death Differ.* 14: 1237–1243.
12. Nicholson, D. W. 1999. Caspase structure, proteolytic substrates, and function during apoptotic cell death. *Cell Death Differ.* 6: 1028–1042.
13. Yamashima, T. 2004. $Ca2^{+}$-dependent proteases in ischemic neuronal death: a conserved "calpain-cathepsin cascade" from nematodes to primates. *Cell Calcium* 36: 285–293.
14. Holler, N., R. Zaru, O. Micheau, M. Thome, A. Attinger, S. Valitutti, J. L. Bodmer, P. Schneider, B. Seed, and J. Tschopp. 2000. Fas triggers an alternative, caspase-8-independent cell death pathway using the kinase RIP as effector molecule. *Nat. Immunol.* 1: 489–495.
15. Sperandio, S., K. Poksay, I. de Belle, M. J. Lafuente, B. Liu, J. Nasir, and D. E. Bredesen. 2004. Paraptosis: mediation by MAP kinases and inhibition by AIP-1/Alix. *Cell Death Differ.* 11: 1066–1075.
16. Liu, J., J. D. Farmer, Jr., W. S. Lane, J. Friedman, I. Weissman, and S. L. Schreiber. 1991. Calcineurin is a common target of cyclophilin-cyclosporin A and FKBP-FK506 complexes. *Cell* 66: 807–815.
17. Bokkerink, J. P., E. H. Stet, R. A. De Abreu, F. J. Damen, T. W. Hulscher, M. A. Bakker, and J. A. van Baal. 1993. 6-Mercaptopurine: cytotoxicity and biochemical pharmacology in human malignant T-lymphoblasts. *Biochem. Pharmacol.* 45: 1455–1463.
18. Legembre, P., S. Daburon, P. Moreau, F. Ichas, F. de Giorgi, J. F. Moreau, and J. L. Taupin. 2005. Amplification of Fas-mediated apoptosis in type II cells via microdomain recruitment. *Mol. Cell. Biol.* 25: 6811–6820.
19. Legembre, P., B. C. Barnhart, L. Zheng, S. Vijayan, S. E. Straus, J. Puck, J. K. Dale, M. Lenardo, and M. E. Peter. 2004. Induction of apoptosis and activation of NF-κB by CD95 require different signalling thresholds. *EMBO Rep.* 5: 1084–1089.
20. Beneteau, M., S. Daburon, J. F. Moreau, J. L. Taupin, and P. Legembre. 2007. Dominant-negative Fas mutation is reversed by down-expression of c-FLIP. *Cancer Res.* 67: 108–115.
21. Scaffidi, C., S. Fulda, A. Srinivasan, C. Friesen, F. Li, K. J. Tomaselli, K. M. Debatin, P. H. Krammer, and M. E. Peter. 1998. Two CD95 (APO-1/Fas) signaling pathways. *EMBO J.* 17: 1675–1687.
22. Legembre, P., P. Moreau, S. Daburon, J. F. Moreau, and J. L. Taupin. 2002. Potentiation of Fas-mediated apoptosis by an engineered glycosylphosphatidylinositol-linked Fas. *Cell Death Differ.* 9: 329–339.
23. Sander, E. E., S. van Delft, J. P. ten Klooster, T. Reid, R. A. van der Kammen, F. Michiels, and J. G. Collard. 1998. Matrix-dependent Tiam1/Rac signaling in epithelial cells promotes either cell-cell adhesion or cell migration and is regulated by phosphatidylinositol 3-kinase. *J. Cell Biol.* 143: 1385–1398.
24. Reid, T., T. Furuyashiki, T. Ishizaki, G. Watanabe, N. Watanabe, K. Fujisawa, N. Morii, P. Madaule, and S. Narumiya. 1996. Rhotekin, a new putative target for Rho bearing homology to a serine/threonine kinase, PKN, and rhophilin in the Rho-binding domain. *J. Biol. Chem.* 271: 13556–13560.
25. Yamada, Y., Y. Natsumeda, and G. Weber. 1988. Action of the active metabolites of tiazofurin and ribavirin on purified IMP dehydrogenase. *Biochemistry* 27: 2193–2196.
26. Glesne, D. A., F. R. Collart, and E. Huberman. 1991. Regulation of IMP dehydrogenase gene expression by its end products, guanine nucleotides. *Mol. Cell. Biol.* 11: 5417–5425.
27. Golstein, P., and G. Kroemer. 2007. Cell death by necrosis: towards a molecular definition. *Trends Biochem. Sci.* 32: 37–43.
28. Kabeya, Y., N. Mizushima, T. Ueno, A. Yamamoto, T. Kirisako, T. Noda, E. Kominami, Y. Ohsumi, and T. Yoshimori. 2000. LC3, a mammalian homologue of yeast Apg8p, is localized in autophagosome membranes after processing. *EMBO J.* 19: 5720–5728.
29. Moubarak, R. S., V. J. Yuste, C. Artus, A. Bouharrour, P. A. Greer, J. Menissier-de Murcia, and S. A. Susin. 2007. Sequential activation of poly-(ADP-ribose) polymerase 1, calpains, and Bax is essential in apoptosis-inducing factor-mediated programmed necrosis. *Mol. Cell. Biol.* 27: 4844–4862.
30. Robert, A., N. Smadja-Lamere, M. C. Landry, C. Champagne, R. Petrie, N. Lamarche-Vane, H. Hosoya, and J. N. Lavoie. 2006. Adenovirus E4orf4 hijacks rho GTPase-dependent actin dynamics to kill cells: a role for endosome-associated actin assembly. *Mol. Biol. Cell* 17: 3329–3344.
31. Prepens, U., I. Just, C. von Eichel-Streiber, and K. Aktories. 1996. Inhibition of Fc epsilon-RI-mediated activation of rat basophilic leukemia cells by *Clostridium difficile* toxin B (monoglucosyltransferase). *J. Biol. Chem.* 271: 7324–7329.
32. Ridley, A. J. 2006. Rho GTPases and actin dynamics in membrane protrusions and vesicle trafficking. *Trends Cell Biol.* 16: 522–529.
33. Dancker, P., I. Low, W. Hasselbach, and T. Wieland. 1975. Interaction of actin with phalloidin: polymerization and stabilization of F-actin. *Biochim. Biophys. Acta* 400: 407–414.
34. Huo, J., R. H. Luo, S. A. Metz, and G. Li. 2002. Activation of caspase-2 mediates the apoptosis induced by GTP-depletion in insulin-secreting (HIT-T15) cells. *Endocrinology* 143: 1695–1704.
35. Hall, A. 1998. Rho GTPases and the actin cytoskeleton. *Science* 279: 509–514.
36. Stowers, L., D. Yelon, L. J. Berg, and J. Chant. 1995. Regulation of the polarization of T cells toward antigen-presenting cells by Ras-related GTPase CDC42. *Proc. Natl. Acad. Sci. USA* 92: 5027–5031.
37. Sperandio, S., I. de Belle, and D. E. Bredesen. 2000. An alternative, nonapoptotic form of programmed cell death. *Proc. Natl. Acad. Sci. USA* 97: 14376–14381.
38. Mathew, R., and E. White. 2007. Why sick cells produce tumors: the protective role of autophagy. *Autophagy* 3: 502–505.
39. Hahn, W. C., and R. A. Weinberg. 2002. Rules for making human tumor cells. *N. Engl. J. Med.* 347: 1593–1603.
40. Igney, F. H., and P. H. Krammer. 2002. Death and anti-death: tumour resistance to apoptosis. *Nat. Rev. Cancer* 2: 277–288.
41. Penn, I. 2000. Cancers in renal transplant recipients. *Adv. Ren. Replace. Ther.* 7: 147–156.
42. Robson, R., J. M. Cecka, G. Opelz, M. Budde, and S. Sacks. 2005. Prospective registry-based observational cohort study of the long-term risk of malignancies in renal transplant patients treated with mycophenolate mofetil. *Am. J. Transplant.* 5: 2954–2960.
43. Ren, Y., J. Tang, M. Y. Mok, A. W. Chan, A. Wu, and C. S. Lau. 2003. Increased apoptotic neutrophils and macrophages and impaired macrophage phagocytic clearance of apoptotic neutrophils in systemic lupus erythematosus. *Arthritis Rheum.* 48: 2888–2897.
44. Iaccarino, L., S. Arienti, M. Rampudda, M. Canova, F. Atzeni, P. Sarzi Puttini, and A. Doria. 2007. Mycophenolate mofetil in lupus glomerulonephritis: effectiveness and tolerability. *Ann. NY Acad. Sci.* 1110: 516–524.